

# Motions of a Powered Top with a Spherical Tip on a Curved Surface

David C. Meeker  
Miles A. Townsend

Shock and Vibrations, 2(1):23-32, Jan. 1995

## Abstract

The purpose of this paper is to model the dynamics of a top with a finite radius tip on a curved basin in a gravitational field without (and with) energy addition and dissipation. This is an extension of a very general and classical problem and requires development of a method for treating the dynamical interactions between the two curved surfaces. The full nonlinear equations of motion are indicated; however, these equations are very complex and do not show the dominant mechanisms which define the system motions. A novel method of “partial linearization” is employed which reduces the equations of motion to a relevant and tractable form in which these mechanisms are clearly exposed. The model and related results are compared with relevant examples from the literature. The movement of the top is simulated by an integration of the fully nonlinear equations of motion and compared with the partially linearized results.

## 1 Introduction

The purpose of this paper is to model the dynamics of a top with a finite radius tip on a curved basin in a gravitational field without (and with) energy addition and dissipation. This study arose from observing the *Top Secret*<sup>®</sup> toy manufactured by Andrews Manufacturing of Eugene, Oregon (Anderson Mfg. (1984)). This is one of those devices which can be invented and manufactured, but whose underlying mechanics and behavior are neither obvious nor easily analyzed. This device features a small top that spins on a shallow plastic bowl. The top appears not to slow over time as it wanders on a non-periodic course throughout the bowl. While the toy is styled to create the illusion of perpetual motion, the top actually is subjected to torque through a brushless motor arrangement. Per Fig. 1, underneath the center of the base are two coils of copper wire around an iron core. A permanent magnet is encased within the spinning top. A simple transistor circuit and battery controls the coils such that there is an applied torque during half of each revolution of the top if the top is suitably close to the coil. Upon further observation, unusual behavior can be observed regardless of whether or not the battery is connected.

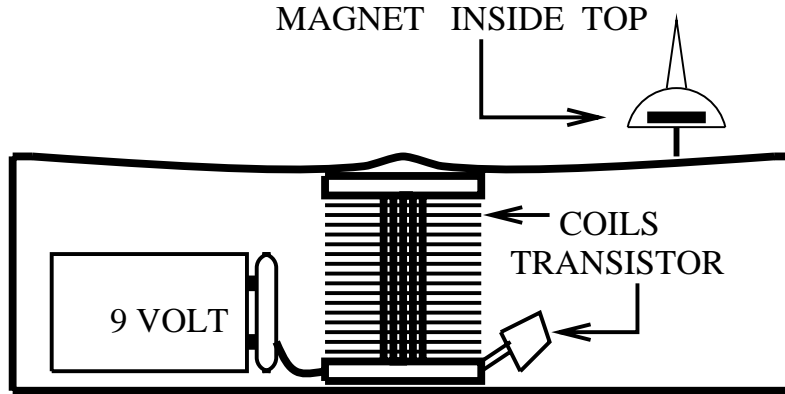


Figure 1: Cross section of the toy's arrangement.

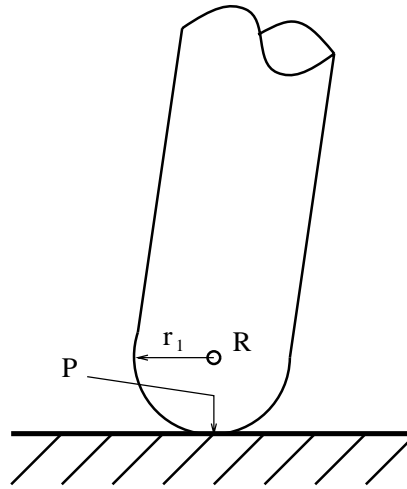


Figure 2: Contact with surface.

## 2 Model Development

Most previous studies assume that the top spins upon a flat, level surface and that the contact with the surface is stationary point contact (for example, Greenwood (1965) and Marion (1965)). Kane and Levinson (1978) model a spherical tip on a flat surface and permit both rolling and sliding behavior. In the present study, the effects of a curved surface on the modeling and motions of the top are examined. Accordingly, in Fig. 2, the contact end of the top is a hemisphere of radius  $r_1$  on the end of a cylinder. Initially, it is assumed that the top rolls without slip on the surface. However, as the problem will be posed, it is easy to solve for the normal and tangential forces to check for possible sliding (i.e., calculate the limiting coefficient of friction). These forces are calculated (in a later section) to validate the assumption of rolling for several specific trajectories.

Five generalized coordinates and generalized speeds are defined pursuant to the development of the equations of motion using Kane's method, as described in Kane and Levinson (1985). In Fig. 3, the five coordinates,  $q_1, \dots, q_5$ , and a surface shape function  $h(q_1, q_2)$  describe the position of the top at time  $t$ . Coordinates  $q_1, q_2$ , and  $h(q_1, q_2)$  denote the  $c_1, c_2$ , and  $c_3$  coordinates respectively of point  $R$  in the top relative to point  $O$  in the fixed reference frame  $C$ . (See Eq. (4) below.)

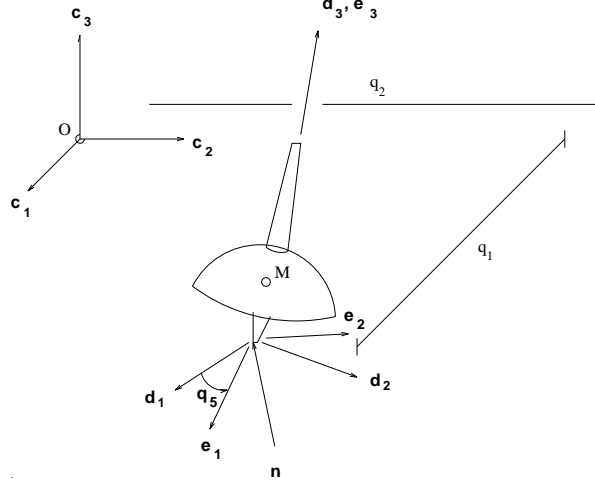


Figure 3: Explanation of reference frames.

Generalized coordinates  $q_3, q_4$ , and  $q_5$  are successive 1,2,3 rotations describing the orientation of reference frame  $E$  fixed in the top with respect to  $C$ . Point  $M$  denotes the mass center of the top.  $M$  lies a distance  $r_2$  away from  $R$  along  $e_3$ .

Five generalized speeds are defined by

$$u_i = \dot{q}_i \quad i = 1, \dots, 5 \quad (1)$$

The rolling condition derived below creates two nonholonomic constraints that eliminate  $u_1$  and  $u_2$ .

The contact point  $P$  is at a distance  $r_1$  away from  $R$  on a line normal to the surface. A surface normal,  $n_o$ , is

$$n_o = (c_1 + \frac{\partial}{\partial q_1} h(q_1, q_2) c_3) \times (c_2 + \frac{\partial}{\partial q_2} h(q_1, q_2) c_3) \quad (2)$$

The unit surface normal is

$$n = \frac{n_o}{|n_o|} = \frac{-\frac{\partial h}{\partial q_1} c_1 - \frac{\partial h}{\partial q_2} c_2 + c_3}{\sqrt{1 + (\frac{\partial h}{\partial q_1})^2 + (\frac{\partial h}{\partial q_2})^2}} \quad (3)$$

The position vector to  $R$  from  $O$  in the  $C$  frame is

$${}^C \mathbf{p}^R = q_1 \mathbf{c}_1 + q_2 \mathbf{c}_2 + h(q_1, q_2) \mathbf{c}_3 \quad (4)$$

The velocity of  $R$  in the  $C$  frame is then

$${}^C \mathbf{v}^R = u_1 \mathbf{c}_1 + u_2 \mathbf{c}_2 + (u_1 \frac{\partial h}{\partial q_1} + u_2 \frac{\partial h}{\partial q_2}) \mathbf{c}_3 \quad (5)$$

An intermediate frame  $D$  moves with the top such that the top ( $E$ ) spins about the common  $\mathbf{d}_3 - \mathbf{e}_3$  axis. A  $C'$  frame is an intermediate frame between  $C$  and  $D$  such that the angular velocity of the  $D$  frame with respect to the  $C$  frame is

$${}^C \boldsymbol{\omega}^D = u_3 \mathbf{c}_1 + u_4 \mathbf{c}'_2 \quad (6)$$

and the angular velocity of the E frame with respect to the C frame is

$${}^C\boldsymbol{\omega}^E = {}^C\boldsymbol{\omega}^D + u_5\mathbf{d}_3 \quad (7)$$

The velocity of the contact point P independent of any motion constraints is

$${}^C\mathbf{v}^P = {}^C\mathbf{v}^R - {}^C\boldsymbol{\omega}^E \times r_1\mathbf{n} \quad (8)$$

For rolling of the top's tip on the surface of the bowl

$${}^C\mathbf{v}^P = 0 \quad (9)$$

Solving Eq. (9) for  $u_1$  and  $u_2$  gives the following nonholonomic motion constraints:

$$u_1 = \frac{r_1(u_4 \cos q_3 - u_5 \cos q_4 \sin q_3 + u_5 \cos q_3 \cos q_4 \frac{\partial h}{\partial q_2} + u_4 \sin q_3 \frac{\partial h}{\partial q_2})}{\sqrt{1 + (\frac{\partial h}{\partial q_1})^2 + (\frac{\partial h}{\partial q_2})^2}} \quad (10)$$

$$u_2 = \frac{r_1(-u_3 - u_5 \sin q_4 - u_5 \cos q_3 \cos q_4 \frac{\partial h}{\partial q_1} - u_4 \sin q_3 \frac{\partial h}{\partial q_1})}{\sqrt{1 + (\frac{\partial h}{\partial q_1})^2 + (\frac{\partial h}{\partial q_2})^2}} \quad (11)$$

Equations (10) and (11) are substituted into Eqs. (5) through (7) and into subsequent equations whenever  $u_1$  or  $u_2$  appear through differentiation of  $q_1$  or  $q_2$ .

The velocity of the top's mass center M in the C frame is then

$${}^C\mathbf{v}^M = {}^C\mathbf{v}^R + {}^C\boldsymbol{\omega}^E \times r_2\mathbf{d}_3 \quad (12)$$

and the acceleration of the mass center is

$${}^C\mathbf{a}^M = {}^C d {}^C\mathbf{v}^M / dt \quad (13)$$

The angular acceleration of the top is

$${}^C\boldsymbol{\alpha}^E = {}^C d {}^C\boldsymbol{\omega}^E / dt \quad (14)$$

${}^C\boldsymbol{\omega}^E$  and  ${}^C\boldsymbol{\alpha}^E$  can be expressed in the D frame as

$${}^C\boldsymbol{\omega}^E = w_1\mathbf{d}_1 + w_2\mathbf{d}_2 + w_3\mathbf{d}_3 \quad (15)$$

$${}^C\boldsymbol{\alpha}^E = \alpha_1\mathbf{d}_1 + \alpha_2\mathbf{d}_2 + \alpha_3\mathbf{d}_3 \quad (16)$$

so that net inertial torque  $\mathbf{T}_I$  about M is

$$\mathbf{T}_I = -(\alpha_1 I_1 - w_2 w_3 (I_1 - I_3))\mathbf{d}_1 - (\alpha_2 I_1 - w_3 w_1 (I_3 - I_1))\mathbf{d}_2 - \alpha_3 I_3 \mathbf{d}_3 \quad (17)$$

where  $I_1$  and  $I_3$  are the principal moments of inertia about  $\mathbf{e}_1$  and  $\mathbf{e}_3$  respectively. The resultant inertial force at M is

$$\mathbf{F}_I = -m {}^C\mathbf{a}^M \quad (18)$$

The nonholonomic generalized inertial forces are then

$$Q_i^* = \frac{\partial^C \mathbf{v}^M}{\partial u_i} \cdot \mathbf{F}_I + \frac{\partial^C \boldsymbol{\omega}^E}{\partial u_i} \cdot \mathbf{T}_I \quad i = 3, 4, 5 \quad (19)$$

The nonholonomic generalized active forces are calculated from

$$Q_i = \frac{\partial^C \mathbf{v}^M}{\partial u_i} \cdot \mathbf{F}_A + \frac{\partial^C \boldsymbol{\omega}^E}{\partial u_i} \cdot \mathbf{T}_A \quad i = 3, 4, 5 \quad (20)$$

$\mathbf{F}_A$  is the externally applied resultant force

$$\mathbf{F}_A = -mg\mathbf{e}_3 \quad (21)$$

where  $m$  is the top's mass and  $g$  is gravitational constant.  $\mathbf{T}_A$  is the external torque at the mass center  $M$ . Initially, the electronic circuit in the top is considered to be inactive, such that

$$\mathbf{T}_A = 0 \quad (22)$$

From Eqs. (19) and (20), the equations of motion (Kane's equations) are

$$Q_i + Q_i^* = 0 \quad i = 3, 4, 5 \quad (23)$$

Equations (10),(11) and (23) describe the motions of the top on a curved surface.

### 3 Special Cases

The equations of motion are formidable in the general case, and it is instructive to consider some special cases. First, consider a flat horizontal surface; hence,  $h(q_1, q_2) = 0$ . Then  $\mathbf{n}$  is equal to  $\mathbf{e}_3$  and Eqs. (10),(11) and (23) become

$$\dot{q}_1 = r_1 u_4 \cos q_3 - r_1 u_5 \cos q_4 \sin q_3 \quad (24)$$

$$\dot{q}_2 = -(r_1 u_3) - r_1 u_5 \sin q_4 \quad (25)$$

$$\begin{aligned} 0 = & gmr_2 \cos q_4 \sin q_3 - \\ & \cos q_4 (I_3 u_4 u_5 + I_1 \cos q_4 \dot{u}_3 - 2I_1 u_3 u_4 \sin q_4 + \\ & I_3 u_3 u_4 \sin q_4) - I_3 \sin q_4 * \\ & (u_3 u_4 \cos q_4 + \dot{u}_5 + \dot{u}_3 \sin q_4) - \\ & mr_2^2 \cos q_4 \sin q_3 (u_3^2 \cos q_3 \cos q_4 + u_4^2 \cos q_3 \cos q_4 + \\ & \cos q_4 \dot{u}_3 \sin q_3 + \cos q_3 \dot{u}_4 \sin q_4 - \\ & 2u_3 u_4 \sin q_3 \sin q_4) - \\ & m(-r_1 - r_2 \cos q_3 \cos q_4) * \\ & (-(r_1 (u_4 u_5 \cos q_4 + \dot{u}_3 + \dot{u}_5 \sin q_4)) + \\ & r_2 (-(\cos q_3 \cos q_4 \dot{u}_3) + u_3^2 \cos q_4 \sin q_3 + \\ & u_4^2 \cos q_4 \sin q_3 + 2u_3 u_4 \cos q_3 \sin q_4 + \end{aligned}$$

$$\begin{aligned}
& \dot{u}_4 \sin q_3 \sin q_4)) \tag{26} \\
0 = & I_1 u_3 u_5 \cos q_4 - I_1 u_3 u_5 \cos^3 q_4 + I_3 u_3 u_5 \cos^3 q_4 - \\
& I_1 \dot{u}_4 + g m r_2 \cos q_3 \sin q_4 + \\
& (-I_1 + I_3) u_3 u_5 \cos q_4 \sin^2 q_4 - \\
& m r_2^2 \cos q_3 \sin q_4 (u_3^2 \cos q_3 \cos q_4 + u_4^2 \cos q_3 \cos q_4 + \\
& \cos q_4 \dot{u}_3 \sin q_3 + \cos q_3 \dot{u}_4 \sin q_4 - \\
& 2 u_3 u_4 \sin q_3 \sin q_4) - \\
& m (r_1 \cos q_3 + r_2 \cos q_4) * \\
& (r_2 \cos q_4 \dot{u}_4 - r_2 u_4^2 \sin q_4 + \\
& r_1 (- (u_3 u_5 \cos q_3 \cos q_4) + \cos q_3 \dot{u}_4 - u_3 u_4 \sin q_3 - \\
& \cos q_4 \dot{u}_5 \sin q_3 + u_4 u_5 \sin q_3 \sin q_4)) - \\
& m r_2 \sin q_3 \sin q_4 (- (r_1 * \\
& (u_4 u_5 \cos q_4 + \dot{u}_3 + \dot{u}_5 \sin q_4)) + \\
& r_2 (- (\cos q_3 \cos q_4 \dot{u}_3) + u_3^2 \cos q_4 \sin q_3 + \\
& u_4^2 \cos q_4 \sin q_3 + 2 u_3 u_4 \cos q_3 \sin q_4 + \\
& \dot{u}_4 \sin q_3 \sin q_4)) + ((-I_1 + I_3) u_3^2 \sin 2 q_4) / 2 \tag{27}
\end{aligned}$$

$$\begin{aligned}
0 = & - (I_3 (u_3 u_4 \cos q_4 + \dot{u}_5 + \dot{u}_3 \sin q_4)) + \\
& m r_1 \cos q_4 \sin q_3 (r_2 \cos q_4 \dot{u}_4 - r_2 u_4^2 \sin q_4 + \\
& r_1 (- (u_3 u_5 \cos q_3 \cos q_4) + \cos q_3 \dot{u}_4 - u_3 u_4 \sin q_3 - \\
& \cos q_4 \dot{u}_5 \sin q_3 + u_4 u_5 \sin q_3 \sin q_4)) + \\
& m r_1 \sin q_4 (- (r_1 (u_4 u_5 \cos q_4 + \dot{u}_3 + \dot{u}_5 \sin q_4)) + \\
& r_2 (- (\cos q_3 \cos q_4 \dot{u}_3) + u_3^2 \cos q_4 \sin q_3 + \\
& u_4^2 \cos q_4 \sin q_3 + 2 u_3 u_4 \cos q_3 \sin q_4 + \\
& \dot{u}_4 \sin q_3 \sin q_4)) \tag{28}
\end{aligned}$$

As a check of the equations, let  $r_1 = 0$ . Equations (24) through (28) describe the classical top with a fixed tip. All dependence upon  $q_1$  and  $q_2$  disappears from the equations of motion;  $q_5$  does not appear in the equations of motion either, since the top is symmetric about the  $e_3$  axis. Equations (26) through (28) are solved for  $\dot{u}_3, \dot{u}_4$  and  $\dot{u}_5$ . The resulting equations are linearized about the upright position, viz.  $q_3 = 0, q_4 = 0, u_3 = 0, u_4 = 0, u_5 = \omega$  (where  $\omega = \text{constant}$ ), to produce the following system:

$$\begin{pmatrix} \dot{q}_3 \\ \dot{q}_4 \\ \dot{u}_3 \\ \dot{u}_4 \end{pmatrix} = \begin{bmatrix} 0 & 0 & 1 & 0 \\ 0 & 0 & 0 & 1 \\ K_1 & 0 & 0 & -G_1 \\ 0 & K_1 & G_1 & 0 \end{bmatrix} \begin{pmatrix} q_3 \\ q_4 \\ u_3 \\ u_4 \end{pmatrix} \tag{29}$$

where

$$K_1 = \frac{g m r_2}{I_1 + m r_2^2} \tag{30}$$

$$G_1 = \frac{I_3 \omega}{I_1 + m r_2^2} \tag{31}$$

|                             |                            |
|-----------------------------|----------------------------|
| mass $m$                    | 2.81 g                     |
| gravitation $g$             | 981 cm/s <sup>2</sup>      |
| $r_1$                       | 0.064 cm                   |
| $r_2$                       | 0.71234 cm                 |
| $I_1$ , Inertia about $e_1$ | 0.583271 g cm <sup>2</sup> |
| $I_3$ , Inertia about $e_3$ | 0.856495 g cm <sup>2</sup> |

Table 1: Measured Top Parameters

This result concurs with previous investigations, such as Webster (1925). The eigenvalues of the above matrix are

$$\lambda = \frac{1}{\sqrt{2}} \left\{ \begin{array}{l} (-G_1^2 + G_1 \sqrt{G_1^2 - 4K_1 + 2K_1})^{1/2} \\ -(-G_1^2 + G_1 \sqrt{G_1^2 - 4K_1 + 2K_1})^{1/2} \\ (-G_1^2 - G_1 \sqrt{G_1^2 - 4K_1 + 2K_1})^{1/2} \\ -(-G_1^2 - G_1 \sqrt{G_1^2 - 4K_1 + 2K_1})^{1/2} \end{array} \right\} \quad (32)$$

The system is marginally stable if the eigenvalues are purely imaginary. This requires that  $G_1^2 - 4K_1 \geq 0$ . Substituting  $K_1$  and  $G_1$  into these expressions, both are satisfied and the top is marginally stable if

$$|\omega| \geq \frac{\sqrt{4mgr_2(I_1 + mr_2^2)}}{I_3} \quad (33)$$

The result corresponds to the ‘‘sleeping top’’ condition for a top near the vertical as described in Greenwood (1965). For this system, moments of inertia and the center of mass were calculated from the measured geometry of the top assuming a constant mass density. These parameters are contained in in Table 1. With these values, Eq. (33) yields  $\omega \geq 146.67 \text{ rad/s}$  (1400.6 RPM) for the top to be stable.

Now, let  $r_1$  be non-zero with  $h(q_1, q_2)$  still equal to zero. By the same procedure as above, the following linearized system of equations is obtained:

$$\begin{Bmatrix} \dot{q}_3 \\ \dot{q}_4 \\ \dot{u}_3 \\ \dot{u}_4 \end{Bmatrix} = \begin{bmatrix} 0 & 0 & 1 & 0 \\ 0 & 0 & 0 & 1 \\ K_2 & 0 & 0 & -G_2 \\ 0 & K_2 & G_2 & 0 \end{bmatrix} \begin{Bmatrix} q_3 \\ q_4 \\ u_3 \\ u_4 \end{Bmatrix} \quad (34)$$

where

$$K_2 = mgr_2/\hat{I}_1 \quad (35)$$

$$G_2 = \omega(I_3 + mr_1(r_1 + r_2))/\hat{I}_1 \quad (36)$$

$$\hat{I}_1 = I_1 + m(r_1 + r_2)^2 \quad (37)$$

$q_1$  and  $q_2$  may be calculated from

$$\dot{q}_1 = -r_1 \omega q_3 + r_1 u_4 \quad (38)$$

$$\dot{q}_2 = -r_1 \omega q_4 - r_1 u_3 \quad (39)$$

Eq. (34) is identical in form to Eq. (29) and thus to the classical top problem with a fixed tip. However, the coefficients are different, and additional equations (38) and (39) exist that depend upon  $q_3, q_4, u_3, u_4$  which describe the motion of point R. In this case, the minimum  $\omega$  allowable for stability is  $134.25 \text{ rad/s}$  ( $1282.0 \text{ RPM}$ ).

## 4 Unpowered Case, Curved Surface

For any flat surface, even if tilted, the normal vector  $n$  is constant, a great simplification. For a curved surface, however,  $n$  changes as a function of  $q_1$  and  $q_2$ , which results in much more complicated equations of motion.

The complete equations of motion for the top were formulated with the aid of a symbolic manipulator. The resulting equations are lengthy and provide little insight into the mechanisms responsible for the top's significant behavior. From observations of the *Top Secret*<sup>®</sup> toy, the top is nearly vertical at all times, even on the curved shell; second, the slope of the bowl is generally quite shallow. Hence, the non-linear dependences on  $q_3, q_4, u_3, u_4$  and on the first derivatives of  $h(q_1, q_2)$  can be linearized about zero in a similar fashion as for the horizontal surface case. The nonlinearities due to the interaction with the curved bowl surface remain. This ‘‘partial linearization’’ greatly reduces the size and complexity of the equations and eliminates terms which normally make little contribution to the toy's behavior:

$$\begin{Bmatrix} \dot{q}_3 \\ \dot{q}_4 \\ \dot{u}_3 \\ \dot{u}_4 \end{Bmatrix} = \begin{bmatrix} 0 & 0 & 1 & 0 \\ 0 & 0 & 0 & 1 \\ K_2 + \frac{\partial^2 h}{\partial q_1^2} K'_2 & \frac{\partial^2 h}{\partial q_1 \partial q_2} K'_2 & \frac{\partial^2 h}{\partial q_1 \partial q_2} G'_2 & -(G_2 + \frac{\partial^2 h}{\partial q_1^2} G'_2) \\ \frac{\partial^2 h}{\partial q_1 \partial q_2} K'_2 & K_2 + \frac{\partial^2 h}{\partial q_2^2} K'_2 & G_2 + \frac{\partial^2 h}{\partial q_2^2} G'_2 & -\frac{\partial^2 h}{\partial q_1 \partial q_2} G'_2 \end{bmatrix} \begin{Bmatrix} q_3 \\ q_4 \\ u_3 \\ u_4 \end{Bmatrix} \quad (40)$$

$$+ \begin{bmatrix} 0 & 0 \\ 0 & 0 \\ \frac{\partial^2 h}{\partial q_1 \partial q_2} K'_2 & B_1 - \frac{\partial^2 h}{\partial q_1^2} K'_2 \\ -B_1 + \frac{\partial^2 h}{\partial q_2^2} K'_2 & \frac{\partial^2 h}{\partial q_1 \partial q_2} K'_2 \end{bmatrix} \begin{Bmatrix} \frac{\partial h}{\partial q_1} \\ \frac{\partial h}{\partial q_2} \end{Bmatrix}$$

$$\dot{q}_1 = r_1 u_4 - \omega r_1 q_3 + \omega r_1 \frac{\partial h}{\partial q_2} \quad (41)$$

$$\dot{q}_2 = -r_1 u_3 - \omega r_1 q_4 + \omega r_1 \frac{\partial h}{\partial q_1} \quad (42)$$

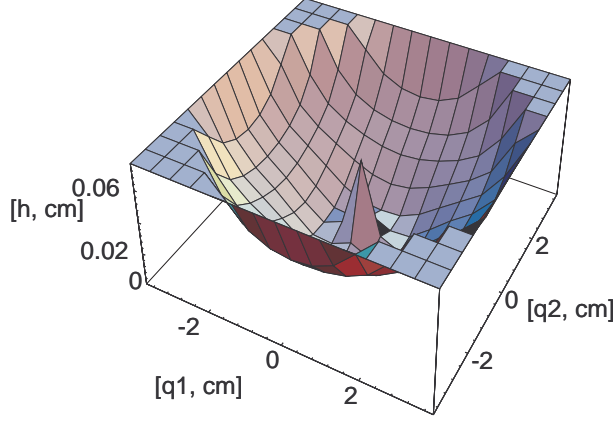


Figure 4: Top Secret bowl shape.

where

$$K'_2 = m r_1^2 \omega^2 (r_1 + r_2) / \hat{I}_1 \quad (43)$$

$$G'_2 = m r_1^2 \omega (r_1 + r_2) / \hat{I}_1 \quad (44)$$

$$B_1 = m g r_1 / \hat{I}_1 \quad (45)$$

These equations exhibit several interesting properties. First, the system does not need to be linearized about  $u_5$ . When the other linearizations are made,  $\dot{u}_5 = 0$ , and  $u_5$  can be taken as  $\omega$ , a constant. Second, the highest derivatives of  $h$  that occur are second derivatives with respect to  $q_1$  and  $q_2$ . Therefore, this method applies in regions where the first and second derivatives of  $h$  are finite.

The “partially linearized” equations (40)-(45) clearly expose the dominant mechanisms responsible for the behavior of the top on curved surfaces for near-vertical orientations. Comparing these equations to Eqs. (34)-(39) for motion on a horizontal surface, additional stiffness and damping terms  $K'_2$  and  $G'_2$  arise in connection with the curvature of the bowl. Forcing terms related to the slope of the bowl are also evident in Eq. (40). Most importantly,  $q_1$  and  $q_2$  are no longer ignorable: these coordinates have a nonlinear influence in all of the equations through the bowl’s shape function,  $h(q_1, q_2)$ . Incidentally, the assumption of shallow slope still allows for significant curvature.

To facilitate a general evaluation of the results, the surface of the *Top Secret*<sup>®</sup> toy’s bowl is approximated (through a least-squares fit to several measured values) by

$$h(q_1, q_2) = 0.0508 - 0.137381 r + 0.119742 r^2 - 0.038818 r^3 + 0.004544 r^4 \quad (46)$$

where

$$r = \sqrt{q_1^2 + q_2^2} \quad (47)$$

See Fig. 4. According to the manufacturer’s literature, Anderson Mfg. (1984), the top usually spins at around 3000 *RPM* (314 *rad/s*). The spin rate of the top may be obtained by measuring the frequency of the current induced in the base coils by the magnet in the spinning top. The top was observed to spin in the neighborhood of 3000 *RPM* while in normal operation. This value will be assumed for  $u_5$  in the following simulations.

| Case | $q_1, cm$ | $q_2, cm$ | $q_3, rad$ | $q_4, rad$ | $u_3, rad/s$ | $u_4, rad/s$ | $u_5, rad/s$ | length, sec |
|------|-----------|-----------|------------|------------|--------------|--------------|--------------|-------------|
| 1    | 3.0       | 0         | 0.1        | 0.2        | 0            | 0            | 314          | 10          |
| 2    | 0.2       | 0         | 0          | 0          | 0            | 0            | 314          | 10          |
| 3    | 1.5       | 0         | 0.05       | 0          | 0            | 0            | 314          | 30          |
| 4    | 0.5       | 1.0       | -0.01      | 0.033      | 0.025        | -0.011       | 314          | 30          |

Table 2: Curved Surface Initial Conditions

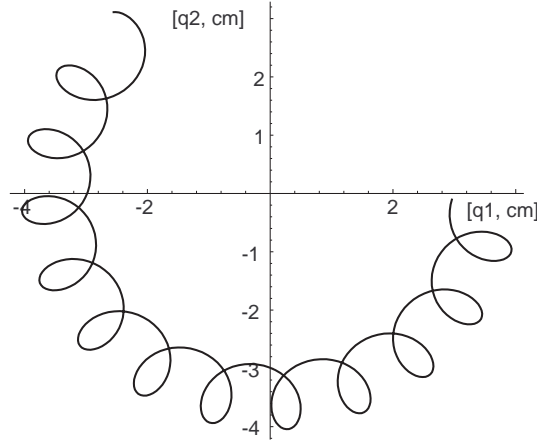


Figure 5: Unpowered Case 1.

A number of cases (initial conditions) were simulated using Eqs. (40)-(45) and a Runge-Kutta integration scheme as described in O’Neil (1987). Figures 5, 6, 7, and 8 show a planar projection of the trajectory of point  $R$ . Axes are graduated in centimeters. Initial conditions are given in Table 2. As a validity test of the linearizing assumptions used to produce Eqs. (40)-(45), the full nonlinear equations were also integrated numerically for the Case 3 initial condition. The trajectory of points augmenting the reduced equations simulation represents the full equations solution. In Case 3, the partially linearized solution agrees very well with the full nonlinear equations simulation over a period of 30 seconds. While the patterns exhibited in the simulations are quite intricate, they seem to always form a repeating pattern that depends upon the initial condition. The patterns are not of the aperiodic nature observed in the actual toy while under power.

## 5 Powered Case, Curved Surface

In the active mode, there is torque on the top due to magnetic attraction and repulsion (per Fig. 1) and an aerodynamic drag effect. The powered case could be formulated by modifying the active force vector  $\mathbf{F}_A$  and the active torque vector  $\mathbf{T}_A$  in Eqs. (22) and (21). However, it is easier to include the effect of these applied forces as a modification of the reduced model used in the unpowered case.

In the unpowered case,  $u_5$  equals zero. For the powered case, a model of the effects of the

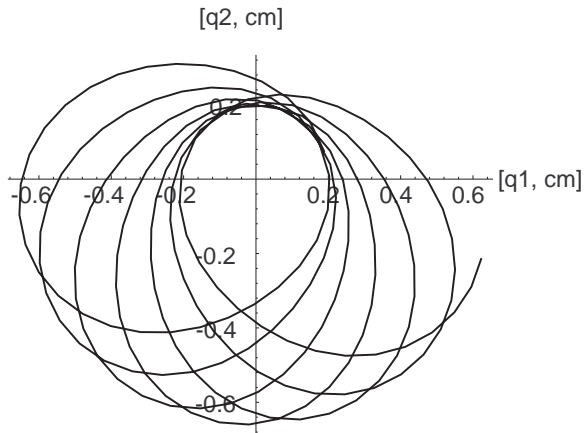


Figure 6: Unpowered Case 2.

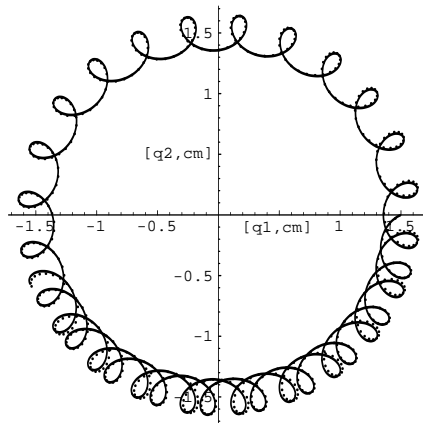


Figure 7: Unpowered Case 3.

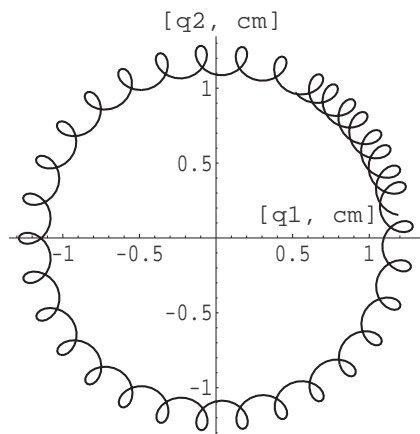


Figure 8: Unpowered Case 4.

magnetics and the air drag would be

$$\dot{u}_5 = \psi(r) - \nu u_5 \quad (48)$$

$\nu$  is the coefficient of aerodynamic drag on the spinner. The torque function  $\psi(r)$  is defined here as

$$\begin{aligned} \psi(r) &= 0, & r \leq r_3 \\ &= \text{constant}/I_3, & r_3 < r < r_4 \\ &= 0, & r \geq r_4 \end{aligned} \quad (49)$$

This model represents a constant torque acting inside a radial band of the bowl in combination with a linear aerodynamic drag on the spinner. This model provides a mechanism for the top to be charged with energy and explore the outer regions of the bowl. When drag slows the top sufficiently, the top will tend back towards the lower sections of the bowl, where it will be energized and repeat the cycle.

An alternate model of  $\psi$  might reflect the inverse-square nature of magnetic force. Also, the magnetic force may weakly torque the spinner about the  $d_1$  and  $d_2$  axes as well as  $d_3$ . In this study, however, the simple model showed an acceptable class of results.

Values for  $r_3$  and  $r_4$  are 0.6 cm and 2.5 cm respectively as estimated from the physical arrangement. A value for the torque constant in Eq. (49) that has been observed to give results qualitatively consistent with the physical setup is about 85 dyne cm. Coefficient  $\nu$  was calculated by assuming a first-order decay of the spin rate. The spin rate of the top was measured via base coil currents at several points in time, and  $\nu$  derived from a fit of these data points to the first-order model. Coefficient  $\nu$  was calculated to be about 0.09 sec<sup>-1</sup>.

Numerical simulations were run for several initial conditions with these parameters. For the purpose of comparison to the unpowered case, the same initial conditions were considered. Figures 9, 10, 11, and 12 show the planar projection of the trajectory of point  $R$ . Axes are graduated in centimeters. Initial conditions are given in Table 2. Again, the Case 3 simulation is augmented by an additional trajectory of points. These points represent the solution of the full nonlinear unpowered equations with the above torque and damping model appended to the equation defining  $\dot{u}_5$ .

These simulations had several interesting results. In Case 1, the top was on a trajectory that did not enter the torqued zone before it slowed down and became unstable. This type of behavior has been observed to occur with the *Top Secret*<sup>®</sup> toy. In the other three cases, the behavior was significantly different as compared to the behavior without power. All three cases displayed the erratic trajectories that are characteristic of the observed behavior of the toy. In Case 3, the partially linearized simulation again compared favorably to the full nonlinear solution.

## 6 Assumption of Rolling.

Kane and Levinson (1978) claim that modeling sliding is important for accurately representing a top with a spherical tip. In the present study, rolling is assumed throughout. The validity of pure rolling is examined by deriving the contact forces as follows. Assuming that a Coulomb friction model applies, rolling occurs if the ratio of friction force to normal force at the tip never exceeds

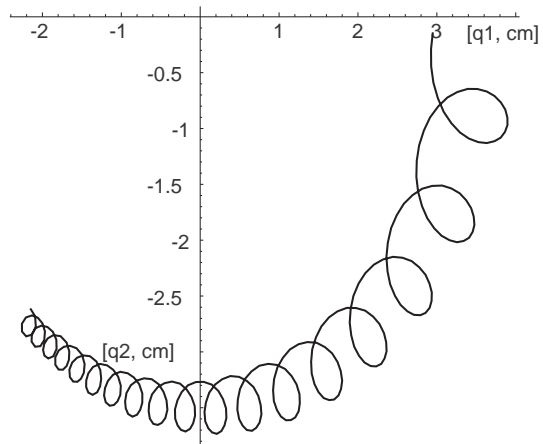


Figure 9: Powered Case 1.

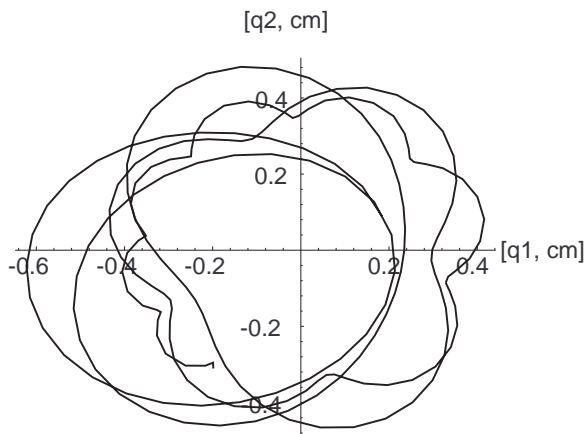


Figure 10: Powered Case 2.

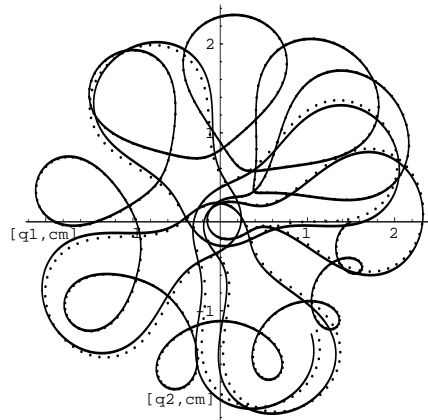


Figure 11: Powered Case 3.

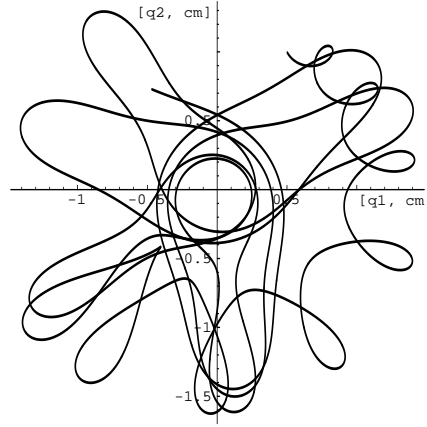


Figure 12: Powered Case 4.

the coefficient of static friction for contact between the top and the surface, *i.e.*

$$\frac{F_f}{F_n} < \mu_s \quad (50)$$

if  $F_f$  is friction force,  $F_n$  is normal force, and  $\mu_s$  is the static coefficient of friction.

To evaluate the contact force, define the additional generalized speed  $u_v$ , such that  ${}^C\mathbf{v}^R$  in Eq. (5) is now

$${}^C\mathbf{v}^R = u_1\mathbf{c}_1 + u_2\mathbf{c}_2 + u_v\mathbf{c}_3 \quad (51)$$

The contact force applied at point  $P$  is denoted as  $\mathbf{Z}$ :

$$\mathbf{Z} = Z_1\mathbf{c}_1 + Z_2\mathbf{c}_2 + Z_3\mathbf{c}_3 \quad (52)$$

Recall Eqs. (8) and (12) for  ${}^C\mathbf{v}^P$  and  ${}^C\mathbf{v}^M$  respectively. Without rolling constraints, partial velocities with respect to  $u_1$ ,  $u_2$ , and  $u_v$  are

| $u_r$ | ${}^C\mathbf{v}^P$ | ${}^C\mathbf{v}^M$ |
|-------|--------------------|--------------------|
| 1     | $\mathbf{c}_1$     | $\mathbf{c}_1$     |
| 2     | $\mathbf{c}_2$     | $\mathbf{c}_2$     |
| $v$   | $\mathbf{c}_3$     | $\mathbf{c}_3$     |

The active force applied at  $P$  is  $\mathbf{Z}$ , and at  $M$  is  $\mathbf{F}_A$  (see Eq. (21)). The inertial force applied at  $M$  is  $\mathbf{F}_I = -m{}^C\mathbf{a}^M$  (Eq. (18)). This implies three equations:

$$\mathbf{F}_A \cdot {}^C\mathbf{v}_r^M + \mathbf{Z} \cdot {}^C\mathbf{v}_r^P + \mathbf{F}_I \cdot {}^C\mathbf{v}_r^M = 0 \quad r = 1, 2, v \quad (53)$$

Denoting  ${}^C\mathbf{a}^M$  as

$${}^C\mathbf{a}^M = a_1\mathbf{c}_1 + a_2\mathbf{c}_2 + a_3\mathbf{c}_3 \quad (54)$$

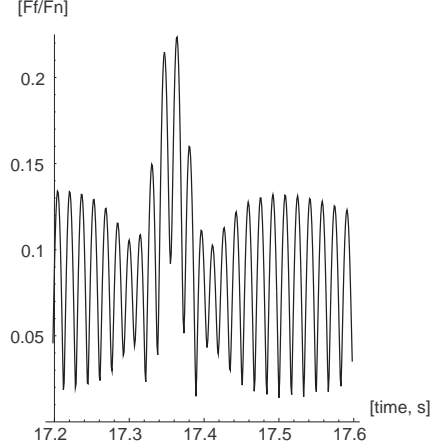


Figure 13: Peak  $F_f/F_n$ , Powered Case 3.

These equations can be solved for  $Z_1$ ,  $Z_2$ , and  $Z_3$ :

$$\begin{aligned} Z_1 &= -ma_1 \\ Z_2 &= -ma_2 \end{aligned} \tag{55}$$

$$Z_3 = -ma_3 + mg \tag{56}$$

When the forces generated during rolling are of interest,  ${}^C\mathbf{a}^M$  is substituted from Eq. 13 (in which the rolling assumptions are included).

The normal force prescribed at the tip is then

$$F_n = \mathbf{Z} \cdot \mathbf{n} \tag{57}$$

where  $\mathbf{n}$  is the outward surface normal defined in equation (3). Friction force is

$$F_f = \sqrt{|\mathbf{Z}|^2 - F_n^2} \tag{58}$$

For ease of computation,  $F_n$  and  $F_f$  were partially linearized as described in Eqs. (39)-(45). The ratio ( $F_n/F_f$ ) was then computed during the entire simulation runs for the powered cases. It was found that peak values occur when the top makes passes close to the center of the bowl – a region where the bowl's slope is comparatively high. Since the unpowered cases never visit this high slope area, they are not considered further.

In extended simulation runs, powered Cases 1 and 2 eventually slow and fall over, implying slippage and violation of linearizing assumptions. These are atypical cases for the toy, since it rarely falls during actual operation. Cases 3 and 4, however, continue indefinitely and represent typical cases. For these typical cases, the maximum values of ( $F_n/F_f$ ) are 0.224 for Case 3 and 0.107 for Case 4. A plot of the peak in Case 3 is illustrated in Fig. 13. Although two cases are not an exhaustive survey, the small magnitude of these peak values indicates that rolling is a reasonable model for the toy under normal circumstances.

## 7 Conclusions

The equations of motion have been developed for the problem of a top with a spherical tip moving without slip across horizontal and curved surfaces. This involved developing methodologies to address the interactions between the curved surfaces, modeling power input and dissipation, and meaningful presentation of results. The assumption of rolling is evaluated and validated for a practical coefficient of static friction.

The evaluation of the stability properties for the classical top problem, to the case of a finite-radius tip on a horizontal surface, to this most general case with a curved surface and power addition and drag losses was addressed by a method herein called “partial linearization.” This involves linearizing only selected terms of the equations of motion, generally involving the principal rotational motions of the top about some observed operating condition. This progression is seen in Eqs. (29)-(31), then (34)-(39), and finally (40)-(45), respectively.

Special cases were evaluated and compared to previous analyses to validate the model formulation. Equations representing the fully nonlinear case on a horizontal plane were produced; subsequently, the effect of a finite-radius tip was evaluated for stability.

A partially linearized model of the top moving on a curved surface without any external energy dissipation or addition was examined. This involves linearizing only those variables which remain “small” while the device is undergoing large motions in the bowl. This enabled the analytical evaluation of the dominant mechanisms and “natural frequencies” of the system. With the assumption of a nearly vertical position for the top, terms embodying the significant interaction with the curved surface were put clearly into evidence. The top followed regular trajectories in this arrangement.

The top was examined moving on a curved surface subject to aerodynamic drag and external torque. The same initial conditions explored in the unpowered case were observed to follow markedly different and seemingly unpredictable trajectories when subject to external forces. Equations (40)-(45) and (48) were proposed as an explanation of the significant behaviors observed from a setup such as the *Top Secret*<sup>®</sup> toy. Under this powered motion model, the nearly vertical orientation of the top as observed in the operating device and assumed in the partial linearization essentially eliminates the possibility of any significant sliding for reasonable values of friction coefficient.

## References

- [1] Andrews Manufacturing Company, 1984, Instruction brochure included with the *Top Secret*<sup>®</sup> toy, Eugene, OR.
- [2] Greenwood, D. T., 1965, *Principles of Dynamics*, Prentice-Hall, Englewood Cliffs, NJ.
- [3] Kane, T. R. and Levinson, D. A., 1978, “A Realistic Solution of the Symmetric Top Problem,” *J. of Applied Mechanics*, Vol. 45, pp. 903-909.
- [4] Kane, T. R. and Levinson, D. A., 1985, *Dynamics: Theory and Applications*, McGraw-Hill, New York.
- [5] Marion, J. B., 1965, *Classical Dynamics of Particles and Systems*, Academic Press, New York.

- [6] O'Neil, P. V., 1987, *Advanced Engineering Mathematics*, Wadsworth Publishing Company, Belmont, CA.
- [7] Webster, A. G., 1925, *The Dynamics of Particles and of Rigid, Elastic, and Fluid bodies; being Lectures on Mathematical Physics*, B. G. Teubner, Leipzig.